












ORIGINAL ARTICLE

OPEN

METTL14 reverses liver fibrosis by inhibiting NOVA2 through an m⁶A-YTHDF2-dependent mechanism

Xiaoxue Hou¹  | Yuwen Li²  | Jiali Song¹  | Linya Peng¹  |
 Wen Zhang¹  | Rui Liu³  | Hui Yuan¹  | Tiantong Feng¹  | Jieying Li³  |
 Wenting Li³  | Chuanlong Zhu^{1,3} 

¹Department of Infectious Disease, The First Affiliated Hospital of Nanjing Medical University, Nanjing, China

²Department of Pediatrics, The First Affiliated Hospital of Nanjing Medical University, Nanjing, China

³Department of Tropical Diseases of the Second Affiliated Hospital, Key Laboratory of Tropical Translational Medicine of Ministry of Education, NHC Key Laboratory of Control of Tropical Diseases, School of Tropical Medicine, Hainan Medical University, Haikou, Hainan, China

Correspondence

Chuanlong Zhu, Department of Infectious Disease, the First Affiliated Hospital of Nanjing Medical University, 300 Guangzhou Rd., Nanjing 210029, PR China.
 Email: zhuchuanlong@jshp.org.cn

Abstract

Background: N⁶-methyladenosine (m⁶A), the most prevalent internal RNA modification in eukaryotic cells, is dynamically regulated in response to a wide range of physiological and pathological states. Nonetheless, the involvement of METTL14-induced m⁶A in liver fibrosis (LF) has yet to be established.

Methods: In vitro, HSC cell lines with knock-down and overexpression of METTL14 were constructed, and the effects of METTL14 gene on the phenotypic function of activated HSCs were observed. The proliferation rate was measured by CCK8 and EDU, the cell proliferation cycle was measured by flow detector, the migration rate was measured by Transwell, and the contractility of F-actin was observed after phalloidin staining. The downstream target gene NOVA2 of METTL14 was screened by combined sequencing of MeRIP-seq and RNA-seq, combined with signal analysis. Adeno-associated virus (AAV) was injected into the tail vein in vivo to knock down the expression of METTL14, so as to further observe the role of METTL14 in the progress of LF.

Results: our research showed that the methylase METTL14 content was decreased in hepatic tissue from patients with LF, leading to a lowered degree of m⁶A modification. Functionally, we discovered that knocking down m⁶A methyltransferase METTL14 led to increased HSC activation and a substantial worsening of LF. Mechanically, as shown in a multiomics study of

Abbreviations: AAV, adeno-associated virus; ALT, alanine aminotransferase; AST, aspartate aminotransferase; DEGs, differentially expressed genes; ECM, extracellular matrix; GEO, Gene Expression Omnibus; KEGG, Kyoto Encyclopedia of Genes and Genomes; LF, liver fibrosis; m⁶A, N⁶-methyladenosine; ns, not significant; RIP, RNA immunoprecipitation; siRNA, small interfering RNA; METTL3, methyltransferase-like 3; METTL14, methyltransferase-like 14; NOVA2, neuro-oncological ventral antigen 2.

Xiaoxue Hou and Yuwen Li contributed equally.

The authors are accountable for all aspects of the work in ensuring that questions related to the accuracy or integrity of any part of the work are appropriately investigated and resolved. The experiments with animals and human samples in this study were conducted according to the principles of the Declaration of Helsinki and approved by the Institutional Animal Care and Use Committee of Nanjing Medical University (Nanjing, China).

Supplemental Digital Content is available for this article. Direct URL citations are provided in the HTML and PDF versions of this article on the journal's website, www.hepcommjournal.com.

This is an open access article distributed under the terms of the Creative Commons Attribution-Non Commercial-No Derivatives License 4.0 (CCBY-NC-ND), where it is permissible to download and share the work provided it is properly cited. The work cannot be changed in any way or used commercially without permission from the journal.

Copyright © 2023 The Author(s). Published by Wolters Kluwer Health, Inc. on behalf of the American Association for the Study of Liver Diseases.

HSCs, depleting METTL14 levels decreased m⁶A deposition on NOVA2 mRNA transcripts, which prompted the activation of YTHDF2 to detect and degrade the decrease of NOVA2 mRNA

Conclusions: METTL14 functioned as a profibrotic gene by suppressing NOVA2 activity in a mechanism dependent on m⁶A-YTHDF2. Moreover, knocking down METTL14 exacerbated LF, while NOVA2 prevented its development and partly reversed the damage.

INTRODUCTION

Nearly 2 million people every year lose their lives due to chronic liver disease, representing 3.5% of all fatalities annually, and roughly 1 million of them are caused by liver cirrhosis and its complications. Cirrhosis of the liver is the 11th major contributor to global mortalities, and there is currently no effective treatment.^[1,2] Early detection and treatment of liver fibrosis (LF) can prevent the progression of liver cirrhosis. Therefore, understanding the pathogenesis of LF is critical for future molecular diagnoses and targeted therapies. LF is a reversible liver injury and repair reaction stimulated by viruses, drugs, inflammation, fat deposition, and other factors. Many inflammatory cytokines, such as IL-6, TNF α , and IL-1 β , as well as profibrosis factors, particularly TGF β 1, are secreted after liver injury to promote HSC activation and proliferation. Activated HSCs proliferate and differentiate into fibroblasts. In addition, activated HSCs produce many collagen fibers that induce extracellular matrix (ECM) deposition. At the same time, lactone drops and vitamin E levels in HSCs decrease, while rough endoplasmic reticulum and microwires increase. These eventually result in LF and further aggravation.^[3–6]

Chemical modification of RNA is an integral part of its apparent regulation. N⁶-methyladenosine (m⁶A) modification is the most prevalent type of RNA alteration in eukaryotes even though ~150 modifications have been documented.^[7,8] The m⁶A modification in mammalian cells is a process that can be reversed and is modulated by “writers,” “readers,” and “erasers” in the m⁶A gene. “Writers” have established m⁶A modifications, including WTAP, METTL3, and METTL14. ALKBH5 and FTO, on the other hand, acted as “erasers,” removing the m⁶A modification. In addition, functional modification of m⁶A requires the recognition of m⁶A modifications by m⁶A readers, including YTHDF1, YTHDF2, YTHDF3, and YTHDC1. m⁶A “readers” regulate the translation and stability of modified RNA.^[9–12]

This investigation on m⁶A modification and LF sought to clarify its function in this disease. Then, we examined the fibrosis-inhibiting effect of the methylases METTL14 and their link to LF. Studies focusing on mechanisms demonstrated that METTL14 is responsible for regulating

the advancement of LF, which is reliant on the m⁶A modification of NOVA2. As per the findings of subsequent analysis, the activity of METTL14 is caused by the regulation of the Wnt/ β -catenin signaling pathway. The results of the present investigation offer a fresh understanding of the possible role that m⁶A modification plays in the advancement of LF.

METHODS

Tissue specimen collection

The control group comprised patients with a hepatic hemangioma or other nonhepatic fibers, and the diseased group comprised patients with hepatitis B-related fibrosis. The Institutional Review Board of the First Affiliated Hospital of Nanjing Medical University granted its approval to the protocol for the research project (approval number: 2022-MD-026). Written consent was obtained from all subjects. Patients' basic information is presented in Supplemental Tables S1, <http://links.lww.com/HC9/A349> and S2, <http://links.lww.com/HC9/A349>.

Cell culture and transfection

Professor Wenting Li donated the LX2 cell line. In an incubator set to 37 °C, cells were grown in a high-sugar DMEM medium containing 10% fetal bovine serum. Primary HSCs were isolated from mouse liver. The cells were naturally activated after being inoculated in a culture dish. The newly separated primary HSCs were subjected to immunofluorescence staining for detecting the specific marker Desmin (Supplemental Figure S2A, <http://links.lww.com/HC9/A445>).

Lentivirus sequence silencing of METTL14 was obtained from Crius (Nanjing, China). Duplex RNAi oligos and overexpression plasmids were also synthesized by Crius (Nanjing, China). Supplemental Tables S3, <http://links.lww.com/HC9/A349> and S4, <http://links.lww.com/HC9/A349>, and S5, <http://links.lww.com/HC9/A349> include the sequencing data that were used for this

investigation. Lipofectamine RNAiMax (Thermo Fisher Scientific) was used to transfect cells for 24 hours with 50 nM small interfering RNAs (siRNAs).

Animals and experimental procedures

The Animal Care and Use Committee of Nanjing Medical University approved all animal experiments. All our operations are in line with ARRIVE statement. The CCl₄-induced LF model was created using male C57BL/6J (20–25 g) mice aged 6–8 weeks. Briefly, the mice were intraperitoneally injected with CCl₄ twice a week for 12 weeks. The control mice received an equivalent amount of oil. shRNA adeno-associated virus (AAV) production and injection: shRNAs were produced for METTL14 and NOVA2 silencing by Jima Co. Ltd. (Supplemental Tables S6, <http://links.lww.com/HC9/A349> and S7, <http://links.lww.com/HC9/A349> display the sequences). Mice received an AAV8 injection of either METTL14 shRNA or NOVA2 shRNA into their tail vein.

qRT-PCR

RT-qPCR with the TB Green FastQC PCR mix was used to detect mRNA expression. The 2^{-ΔΔCt} method was utilized to obtain the relative expression, and the primer sequence is depicted in Supplemental Tables S8, <http://links.lww.com/HC9/A349> and S9, <http://links.lww.com/HC9/A349>.

Western blotting

After lysis of the tissues in precooled radioimmunoprecipitation assay buffer, 40 μg of protein were electrophoresed and transferred to a membrane. Next, the antibody was incubated at 4°C overnight. Finally, a chemiluminescent substrate was used for imaging, and the gray scale of the protein band was photographed for quantitative analysis to determine the relative protein expression levels. Cell Signaling Technology (Danvers, MA) supplied the primary antibodies used in this study, including YTHDF2, Wnt, β-Catenin, GSK3β, and all the secondary antibodies. Proteintech (Wuhan, China) provided primary antibodies against α-SMA, collagenI, METTL3, METTL14 ALKBH5, FTO, WTAP, and NOVA2.

Enzyme-linked immunosorbent assay

We used an ELISA kit (LinkTech Biotechnology, Hangzhou, China) and followed the directions provided by the manufacturer to assess the inflammatory factors

in the serum. A full wavelength microplate reader measured the absorbance at 450 nm.

Biochemical analysis

Following the guidelines of the manufacturer of the liver function analysis kit (Nanjing Chengjian Institute of Bioengineering, China), we measured the levels of alanine aminotransferase and aspartate aminotransferase. (The reference value of the normal range of mouse serum in this kit: alanine aminotransferase: 8.248 ± 5.509; aspartate aminotransferase: 20.155 ± 9.242.) A full wavelength microplate reader measured the absorbance 450 and 630 nm.

Detection of LX2 cell proliferation using EdU and CCK-8 experiments

Transfected LX2 cells were inoculated into 24-well plates (2 × 10⁴ cells/well) and subjected to culturing for 24 hours. Next, EdU solution (100 μL) was introduced into the 24-well plate, followed by 2 hours of incubation. The stained cells were photographed and examined using a microscope. Thereafter, the inoculation of cells was performed in 96-well plates (1000 cells/well). Following the addition of 10 μL of CCK-8 to each well, the optical density at 450 nm was determined.

Cell cycle assay

The cells were stained using a cell cycle staining kit (70-CCS012, MultiSciences, China). Flow cytometry was used to quantify cell counts, and Cell Quest Modfit was used to interpret the data.

Quantification of RNA m⁶A

The EpiQuik m⁶A RNA methylation quantitative kit was utilized to measure m⁶A abundance in mRNA in compliance with the guidelines of the manufacturer (Epigentek, Farmingdale, NY). The enhanced signal was determined by reading the absorbance at 450 nm.

MeRIP-seq and MeRIP-qPCR

The MeRIP tests were performed following the protocol stipulated by the supplier. We fragmented a total of 100 μg of shMETTL14 and shNC RNA into fragments ranging from 100 to 150 bp. After that, about one-tenth of the RNA fragment was used as input. Lianchuan (Hangzhou, China) performed the sequencing on the samples. To

perform MeRIP-qPCR, the methylated RNA that was purified in the previous stages underwent reverse transcription before being subjected to qPCR analysis.

RNA immunoprecipitation assays

LX2 cells were lysed with lysis buffer from the Magna RNA immunoprecipitation (RIP) RNA-binding protein immunoprecipitation kit (Millipore, Bedford, MA). At 4°C, antibodies against magnetic bead proteins A/G, METTL14, IgG, and YTHDF2 were introduced and subjected to incubation for a full night. The next day, RNA was obtained after repeated rinsing and other procedures. The data were processed according to the qPCR treatment described above.

RNA and protein stability assays

The media for the culture was supplemented with actinomycin D at a concentration of 5 µg/mL. At 0, 3, 6, and 9 hours, RNA was extracted from the cells and then examined by qPCR. The growth medium was added with cycloheximide (100 µg/mL). Proteins were isolated from cells at 0, 3, 6, and 9 hours and analyzed by western blotting.

Immunohistochemistry

After the embedded liver tissue sections were incubated with primary antibodies against METTL14, NOVA2, and α -SMA, random images were captured with a microscope (Nikon, Japan). Positively stained cells were counted according to the standard method to evaluate the expression of detected genes.

Immunofluorescence staining

After antigen repair of liver sections, 0.5% polyethylene glycol octylphenyl ether (Triton X-100) was allowed to permeate for 10 minutes, and the sections were washed with phosphate-buffered saline buffer 3 times. Five percent BSA covered the tiled liver sections, sealed at room temperature for 30 minutes, and washed the sections with phosphate-buffered saline buffer solution 3 times; the primary antibody (METTL14 Sigma-Aldrich, USA) was combined with the mouse liver tissue section at 4°C overnight, and the secondary antibody was incubated at 37°C for 2 hours. The section was covered with DAPI staining solution for 5 minutes to stain the nucleus again, and the section was washed with phosphate-buffered saline buffer solution 3 times. Finally, the antifluorescence quencher was sealed and covered with cover glass. Observe and take photographs with a fluorescent microscope.

Transwell cell invasion assay

Herein, 300 µL cell suspension was charged into chambers, 700 µL of the chamber containing 20% fetal bovine serum was charged, and the bottom cells were stained with crystal violet after 24 hours. We selected 5 areas at random and counted the number of cells observed underneath the microscope.

Luciferase reporter system construction

The m⁶A point mutation plasmid was designed according to the motif sequence (Supplemental Table S10, <http://links.lww.com/HC9/A349>, for the plasmid sequence). After the plasmid was transfected, a multi-functional microplate reader was used for detection as directed by the manufacturer.

Cytoskeleton staining

A 12-well plate was used to inoculate the cells that were either knocked down or overexpressed. Then, phalloidin was applied to stain the cytoskeleton in compliance with the guidelines stipulated by the manufacturer. Finally, DAPI staining solution was used to redye the nuclei, and the film was sealed and fixed. A confocal microscope was used to capture the images.

Statistical analysis

Data were analyzed using Prism 9.0 and SPSS 25.0, and expressed as mean \pm SEM or mean \pm SD. An unpaired 2-tailed Student *t* test between 2 groups and a 1-way ANOVA accompanied by a Bonferroni post-test were utilized to examine all of the experimental data. All experiments were repeated at least thrice. Statistical significance was set at $p < 0.05$.

RESULTS

Abnormalities in m⁶A modification and METTL14 downregulation in LF

The differential expression of m⁶A modification enzymes was identified between LF samples and normal hepatic tissue samples using a publicly available clinical database, which shed light on the potential function of the m⁶A modification in LF. After analyzing three different Gene Expression Omnibus (GEO) data sets (GSE36411, GSE77627, and GSE49541), we discovered that the METTL14 expression level was considerably lower in LF than in normal tissues (Figure 1A–C). Subsequently, qRT-PCR and western

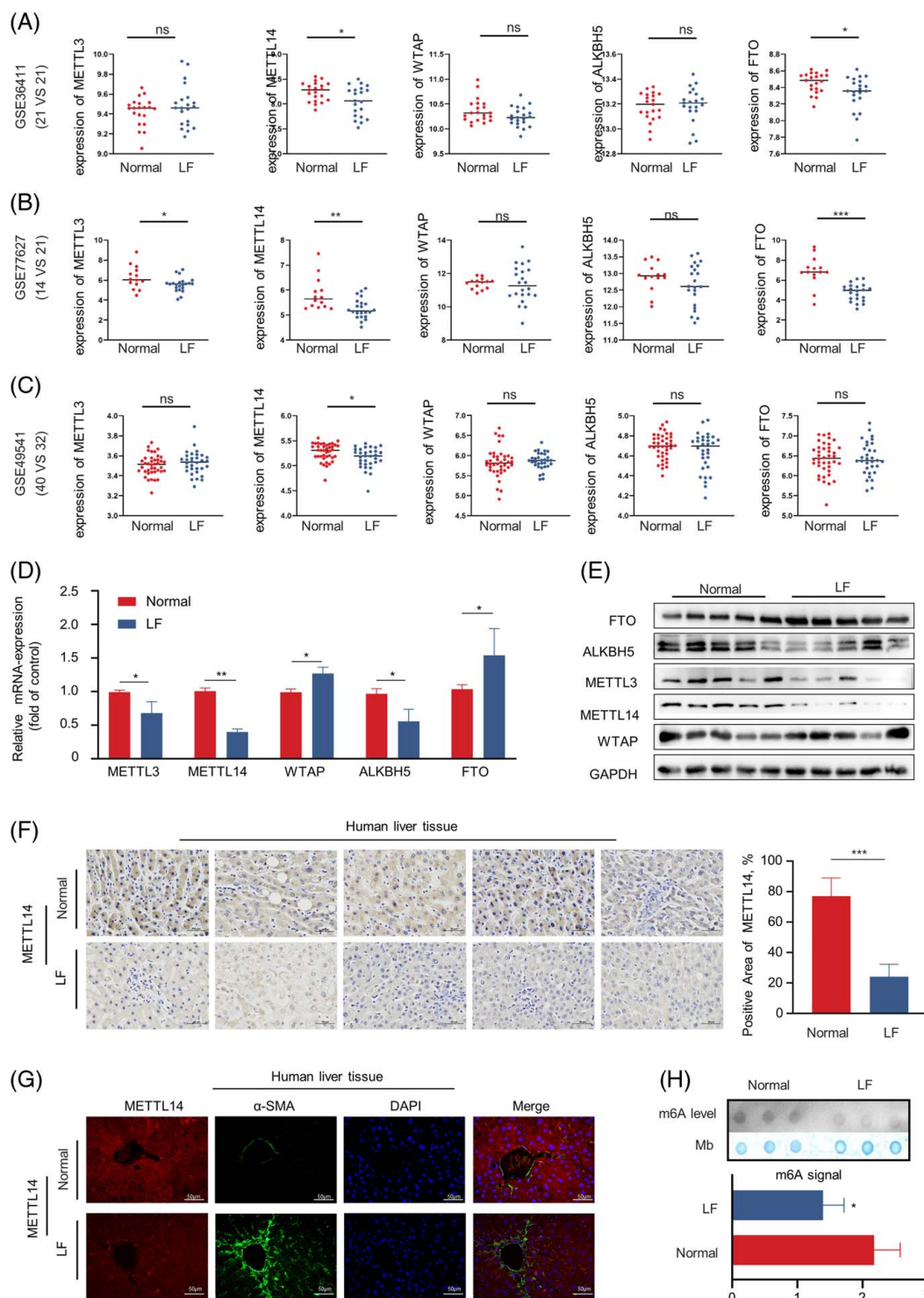


FIGURE 1 m⁶A modification and METTL14 downregulation in LF. (A–C) Expression of METTL14 in LF and its matched normal liver tissues from the GEO database. (D) Relative expression levels of methylase and demethylase of liver tissues from LF and normal liver tissues as determined by qRT-PCR. (E) The expression levels of methylase and demethylase of liver tissues from LF and normal liver tissues as determined by western blotting. (F) METTL14 expression determined by immunohistochemistry in human LF patients (n = 5) and health control (n = 5). Scale bars: 50 μ m. (G) Immunostaining in human liver tissues of patients with LF and control (red: METTL14, green: α -SMA, and blue: DAPI). Scale bar: 50 μ m. (H) Global m⁶A levels in liver mRNA were detected by dot blot; data are presented as the mean \pm SD. * p < 0.05; ** p < 0.01; and *** p < 0.001 (student t test). Abbreviations: GEO, Gene Expression Omnibus; LF, liver fibrosis; m⁶A, N⁶-methyladenosine; ns, not significant.

blotting were conducted to assess the levels of m⁶A modification enzymes in liver tissue samples from LF patients. As per the findings, METTL14 expression was shown to be downregulated in the liver's fibrous tissue (Figure 1D, E). Moreover, we performed immunohistochemistry staining on liver tissue from LF (n=5) and normal liver tissue (n=5). The staining results showed low expression of METTL14 in liver tissue samples from patients with LF (Figure 1F). The results of immunofluorescence staining also proved this point again (Figure 1G). In addition, the overall level of m⁶A was shown to be decreased in fibrous liver tissue in contrast with the level found in control liver tissues (Figure 1H). We created a mouse model of LF by i.p. injection of CCL₄ (Supplemental Figure S1A–E, <http://links.lww.com/HC9/A444>) and found that the liver tissue of fibrotic mice showed low expression of METTL14 (Supplemental Figure S1F, <http://links.lww.com/HC9/A444>). In addition, we found a decrease in m⁶A content during HSCs activation, which was associated with a low level of METTL14 expression (Supplemental Figure S2B–E, <http://links.lww.com/HC9/A445>). Based on these results, METTL14 is remarkably downregulated in fibrous liver tissue, which implies that it could have a role in the modulation of LF advancement through m⁶A modification.

METTL14 promotes the activation of HSCs and the progression of LF

We created the stable METTL14 knockdown based on LX2 cell lines and primary HSCs to examine the function that METTL14 performs in LF (Figure 2A). As expected, METTL14 knockdown significantly decreased m⁶A levels in activated LX2 cells and primary HSCs (Figure 2B). Furthermore, we observed an increase in ECM deposition in LX2 cells and primary HSCs after METTL14 knockdown (Figure 2C). We discovered that depleting METTL14 substantially increased the proliferative rate of LX2 cells and primary HSCs (Figure 2D, E, Supplemental Figure S4A, B, <http://links.lww.com/HC9/A447>). Cell cycle experiments were conducted to provide more evidence that METTL14 plays a role in the proliferation of cells. In METTL14 knockdown cell lines, the findings revealed that the proportion of cells in the G2 phase was reduced, whereas that in the G0/G1 phase was elevated (Figure 2D). In addition, in a transwell migration experiment, the capacity of LX2 cells and primary HSCs to migrate was considerably enhanced when the METTL14 gene was knocked down (Supplemental Figure S5A, <http://links.lww.com/HC9/A448>). The cytoskeleton stained by phalloidin also revealed that the contractility of LX2 cells and primary HSCs F-actin increased after knocking down METTL14 (Supplemental Figure S6A, <http://links.lww.com/HC9/A449>). In addition, we found that overexpression of

METTL14 weakens the activation of HSCs (Supplemental Figure S3A–H, <http://links.lww.com/HC9/A446>). CCL₄-induced LF is a well-established model to investigate LF *in vivo*. To further explore the effect of METTL14 on the progress of LF, we knocked down METTL14 *in vivo* by injecting AAV8-sh-METTL14 through the tail vein (Figure 2F). We discovered that, in contrast with the nontarget control mice, the liver damage of mice knocked down with METTL14 (Figure 2G, H) was more serious (Figure 2I), the liver collagen deposition increased (Figure 2J, K), the level of transaminase increased (Figure 2L), and the level of serum inflammatory factors also increased (Figure 2M). Altogether, our findings indicate that METTL14 is critical for the development of LF.

NOVA2 was shown to be a direct target of METTL14 via RNA-seq and MeRIP-seq analyses

We found that METTL14 suppressed LF advancement in the present research. We used shNC-LX2 and shMETTL14 LX2 cells to perform multigroup sequencing, examine the involvement of METTL14 in the pathogenesis of LF, and identify its downstream targets. The most common m⁶A motif in the peak was AACCC (Figure 3A). MeRIP-seq analysis revealed that the m⁶A signal was primarily concentrated in the 3'-UTR (Figure 3B, C). The findings revealed that the m⁶A peak of 15 genes was downregulated compared with the control group, while the mRNA expression was upregulated. Five m⁶A peaks were upregulated, mRNA expression was upregulated, 4 m⁶A peaks were downregulated, and 13 m⁶A peaks were upregulated, but mRNA expression was downregulated (Figure 3D, E). We discovered that the differential genes were associated with cell cycle, cell proliferation, and EMT pathway after Gene Ontology and Kyoto Encyclopedia of Genes and Genomes enrichment analyses (Figure 3F, G). The differential gene Neuro-Oncological Ventral Ag 2 (NOVA2) is an alternative splice regulator associated with angiogenesis. NOVA2 can affect the structure and function of blood vessels by affecting the polarity of endothelial cells and lumen formation.^[13–15] After METTL14 knockdown, the mRNA expression of NOVA2 increased compared with that in the control group, while the m⁶A peak decreased. Also, the expression of METTL14 was shown to be inversely associated with that of NOVA2 in developing LF, as determined by bioinformatics analysis (Figure 3H). In addition, NOVA2 expression increased during LF progression (Supplemental Figure S7A–D, <http://links.lww.com/HC9/A450>). Therefore, based on preliminary data, we decided to focus our attention on NOVA2 as a candidate targeting gene modified by METTL14 m⁶A.

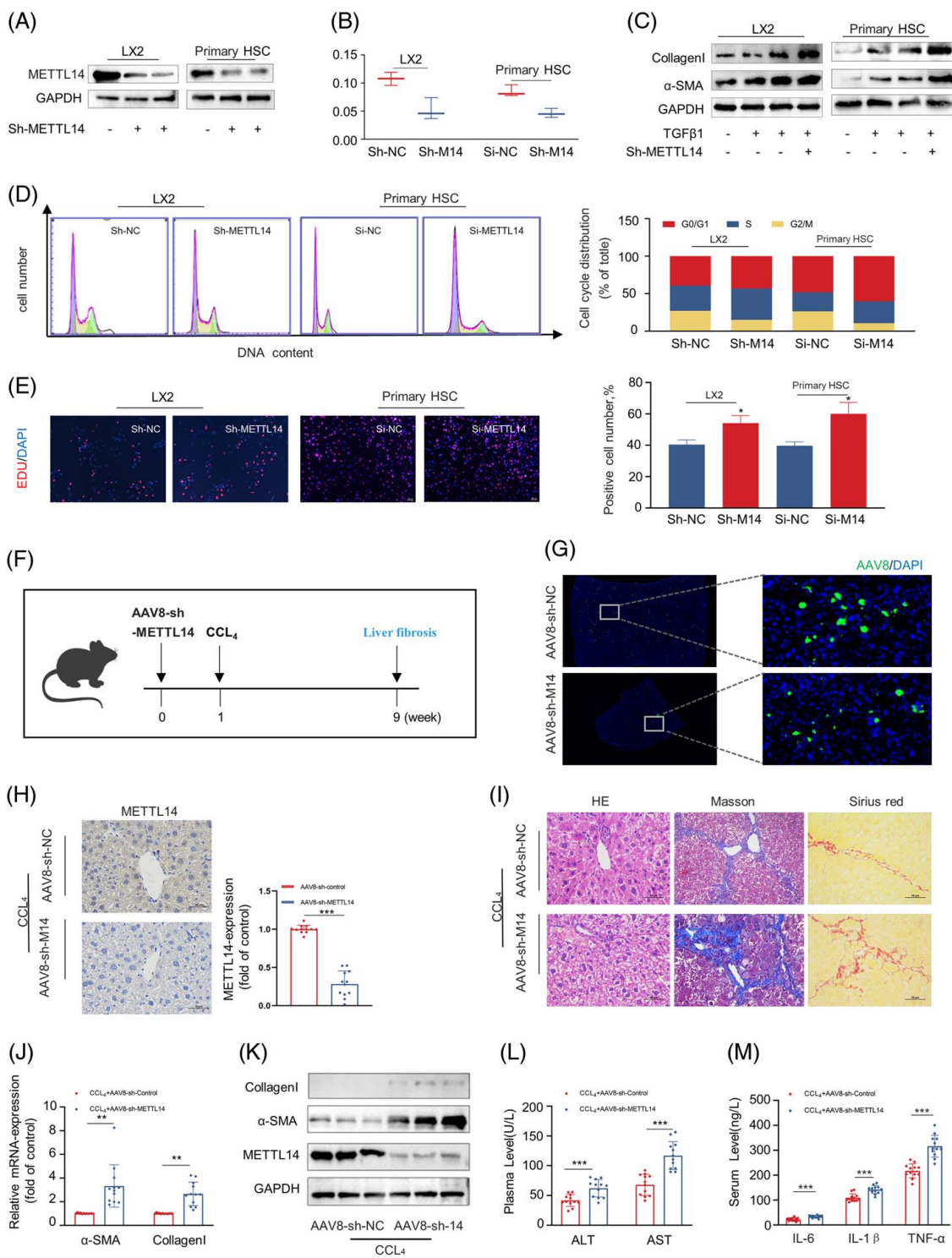


FIGURE 2 METTL14 deficiency promotes HSCs activation and LF. (A) The METTL14 knockdown effect was confirmed at both the mRNA and protein levels. (B) METTL14 knockdown significantly reduced the mRNA m⁶A level in LX2 cells and primary HSCs. (C) Increased ECM accumulation. (D) Cell cycle assays and the calculated LX2 cell and primary HSCs percentages in each phase. (E) LX2 cell and primary HSCs proliferation assessed by EDU; METTL14 knockdown significantly promoted the proliferation rate of HSCs. (F) Protocol for CCL₄-induced LF in a mouse model after tail vein injection of AAV8-sh-METTL14. (G) Fluorescence sections of the liver infected with the adeno-associated virus. (H) METTL14 immunohistochemistry was used to verify the transfection efficiency (n = 12). Scale bars: 50 μm. (I) pathological sections of the liver. (J, K) METTL14 knockdown increased ECM in mouse liver (n = 12). (L) After METTL14 knockdown, increased ALT and AST levels in mice (n = 12). (M) After METTL14 knockdown, increased levels of inflammatory factors in mice (n = 12). Data are presented as the mean ± SD. **p* < 0.05; ***p* < 0.01; and ****p* < 0.001 (Student *t* test). Abbreviations: AAV, adeno-associated virus; ALT, alanine aminotransferase; AST, aspartate aminotransferase; ECM, extracellular matrix; LF, liver fibrosis; m⁶A, N⁶-methyladenosine..

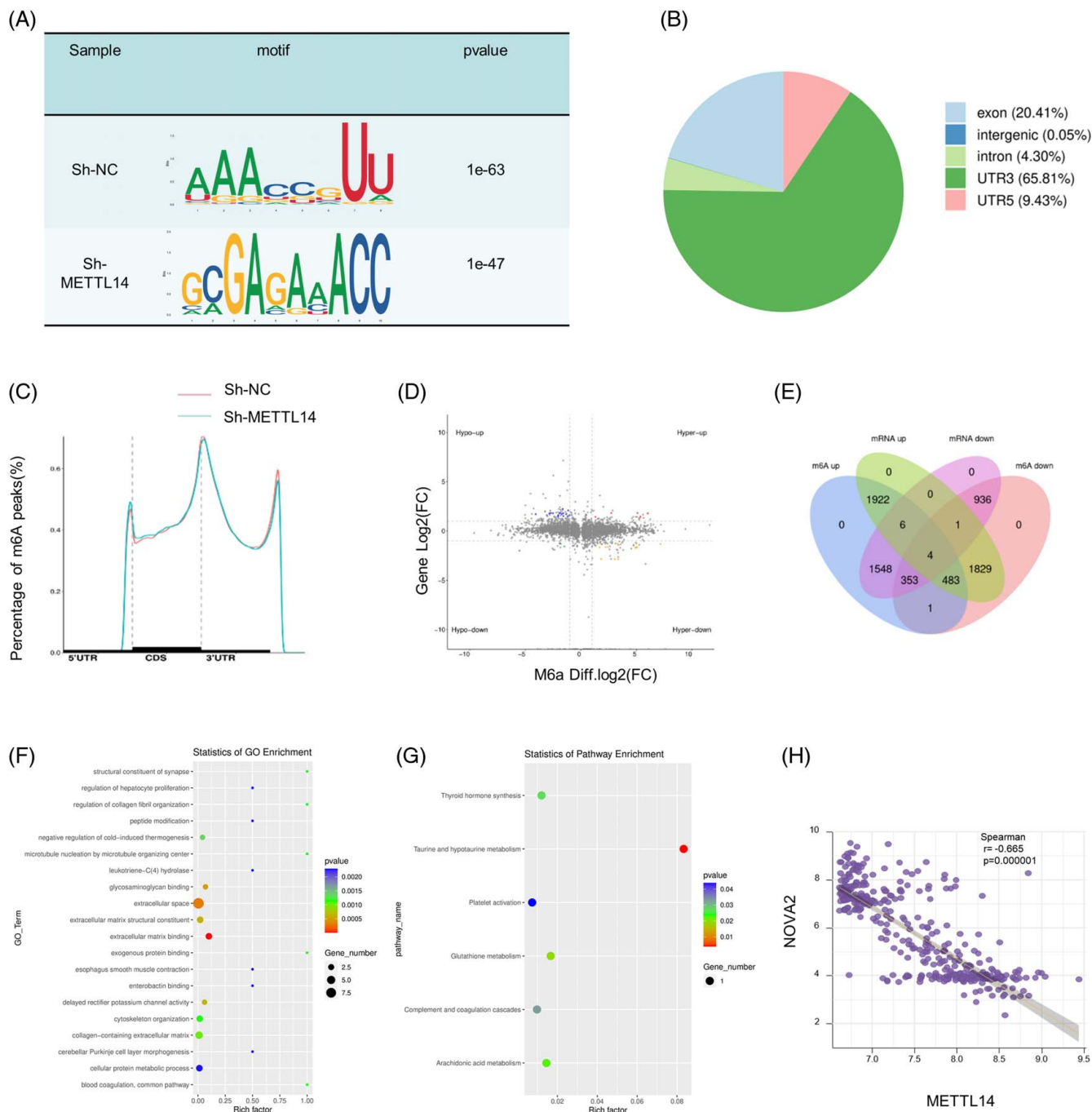


FIGURE 3 Identification of METTL14 targets using RNA-seq and MeRIP-seq. (A) The consensus motif of LX2 cells identified by MeRIP-seq (shNC, $p = 1e-63$; sh-METTL14, $p = 1e-47$). (B, C) The m⁶A signals were largely enriched in 3'-UTR. (D) Four-quadrant diagram of DEGs identified by RNA-seq and MeRIP-seq in shNC and shMETTL14 LX2 cells. Gray, unchanged genes [$|\log_2(\text{fold change})| < 2$ or $p > 0.05$] when comparing the shNC and shMETTL14 groups. Hyper-up, upregulated m⁶A peak and mRNA expression; Hyper-down, m⁶A peak upregulated, mRNA expression downregulated; Hypo-up, m⁶A peak downregulated, mRNA expression upregulated; and Hypo-down, downregulated m⁶A peak, and mRNA expression. (E) Venn diagram of DEGs identified by RNA-seq and MeRIP-seq in shNC and shMETTL14 LX2 cells. (F) GO analysis. (G) KEGG analysis. (H) Correlation between METTL14 and NOVA2 expression in LF patients. Data are presented as the mean \pm SD. * $p < 0.05$; ** $p < 0.01$; and *** $p < 0.001$ (Student *t* test). Abbreviations: DEGs, differentially expressed genes; KEGG, Kyoto Encyclopedia of Genes and Genomes; m⁶A, N⁶-methyladenosine.

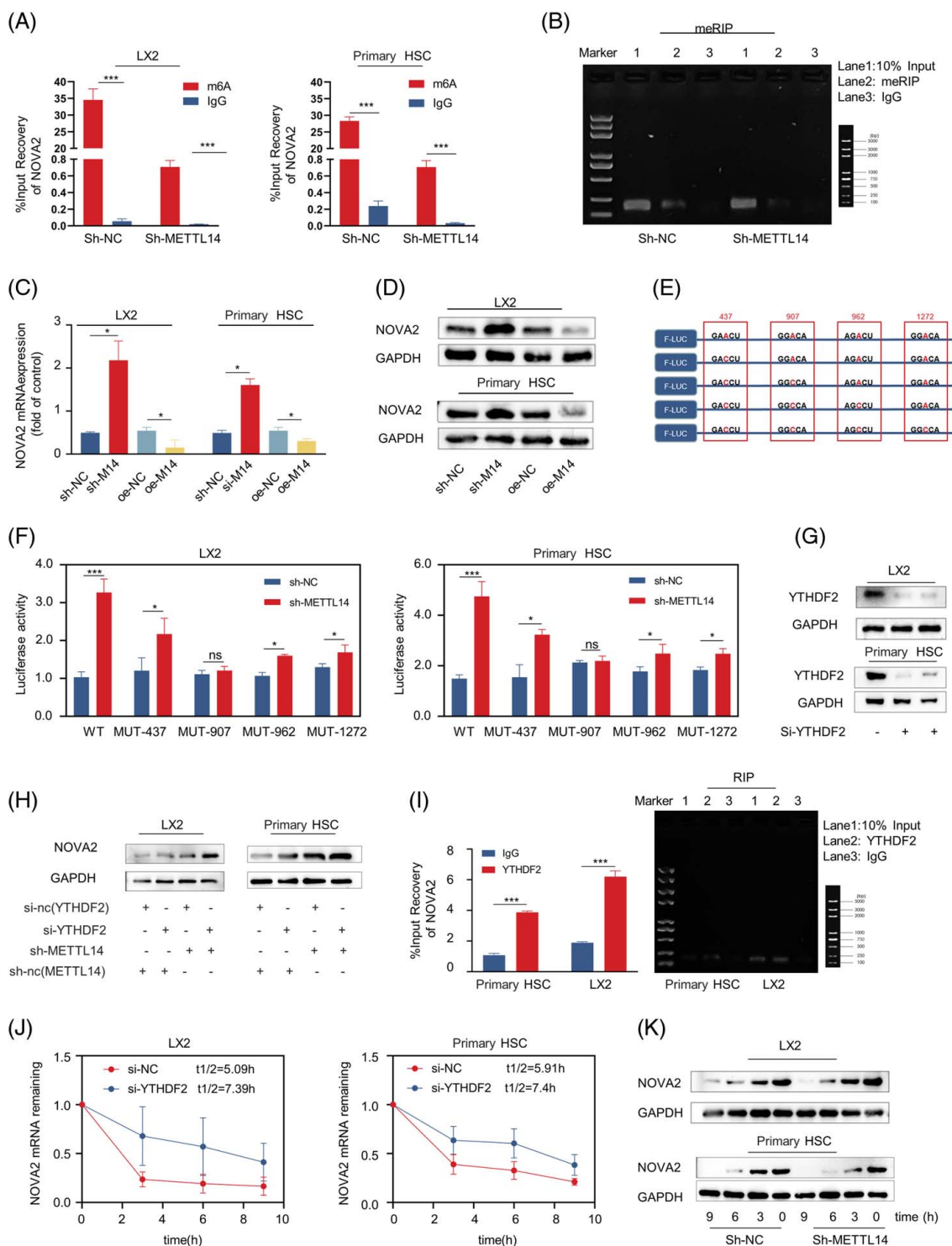


FIGURE 4 NOVA2 mRNA is regulated by METTL14-mediated m⁶A modification through the m⁶A reader YTHDF2. (A, B) The relative m⁶A enrichment of NOVA2 determined by MeRIP-qPCR. (C) The mRNA level of NOVA2 when knocking down or overexpressing METTL14 in LX2 cells and primary HSCs. (D) The protein level of NOVA2 when knocking down or overexpressing METTL14 in LX2 cells and primary HSCs. (E) Schematic representation of mutation in m⁶A sites. (F) Double luciferase gene report. (G) YTHDF2 knockdown in LX2 cells and primary HSCs. (H) YTHDF2 knockdown significantly increased NOVA2 expression. (I) RIP assays of LX2 cells showing the direct binding of YTHDF2 and NOVA2. (J) The stability of NOVA2 protein expression was determined at 0, 3, and 6 hours after knockdown LX2 cells were treated with cycloheximide (5 μg/mL) in METTL14. (K) The decay rate of NOVA2 mRNA when inhibiting YTHDF2 with targeted siRNAs at 0, 3, and 6 hours after actinomycin D (5 μg/mL). Data are presented as the mean ± SD. *p < 0.05; **p < 0.01; and ***p < 0.001 (Student *t* test). Abbreviations: m⁶A, N⁶-methyladenosine; NOVA2, neuro-oncological ventral antigen 2; RIP, RNA immunoprecipitation; siRNA, small interfering RNA.

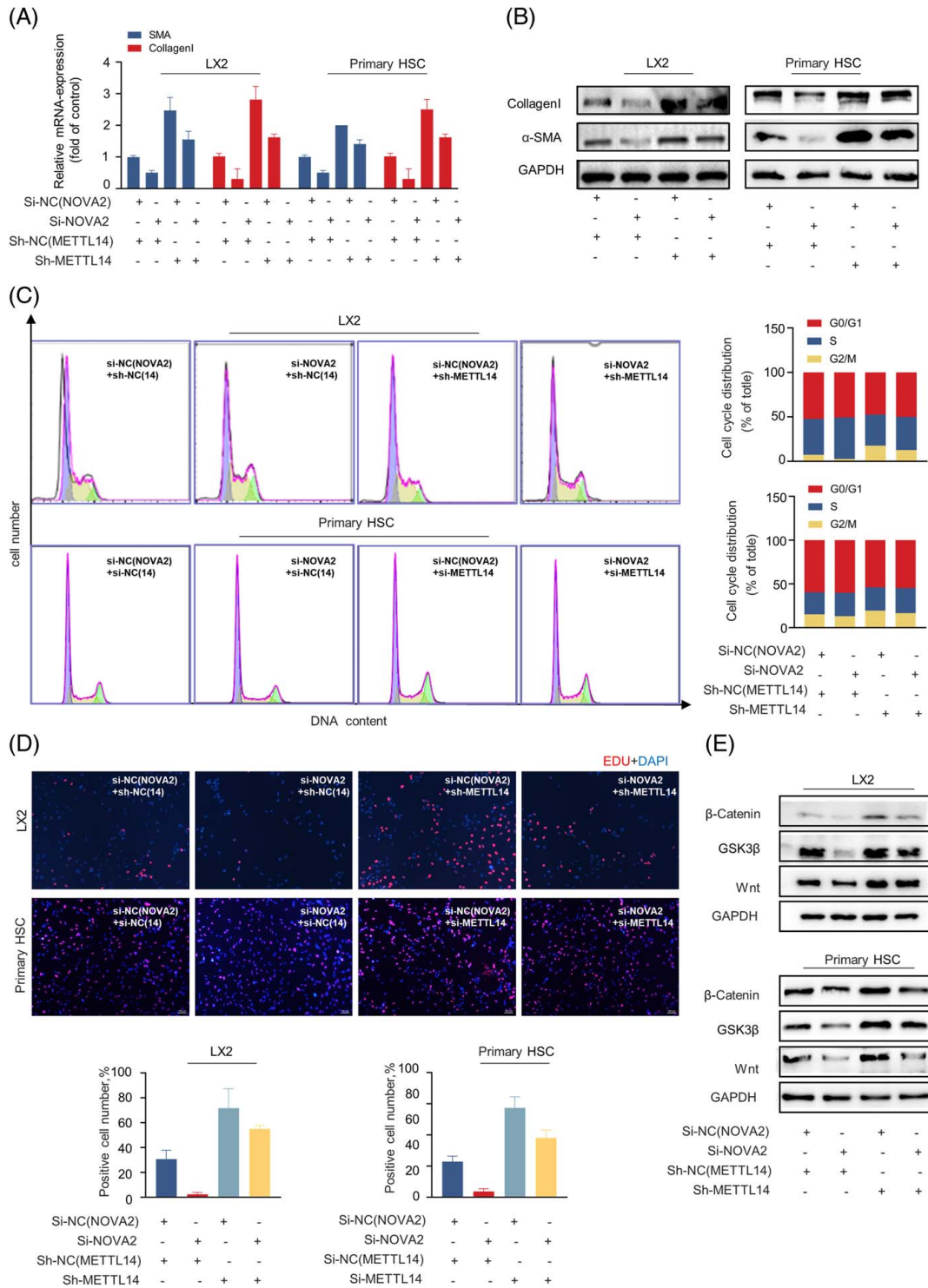
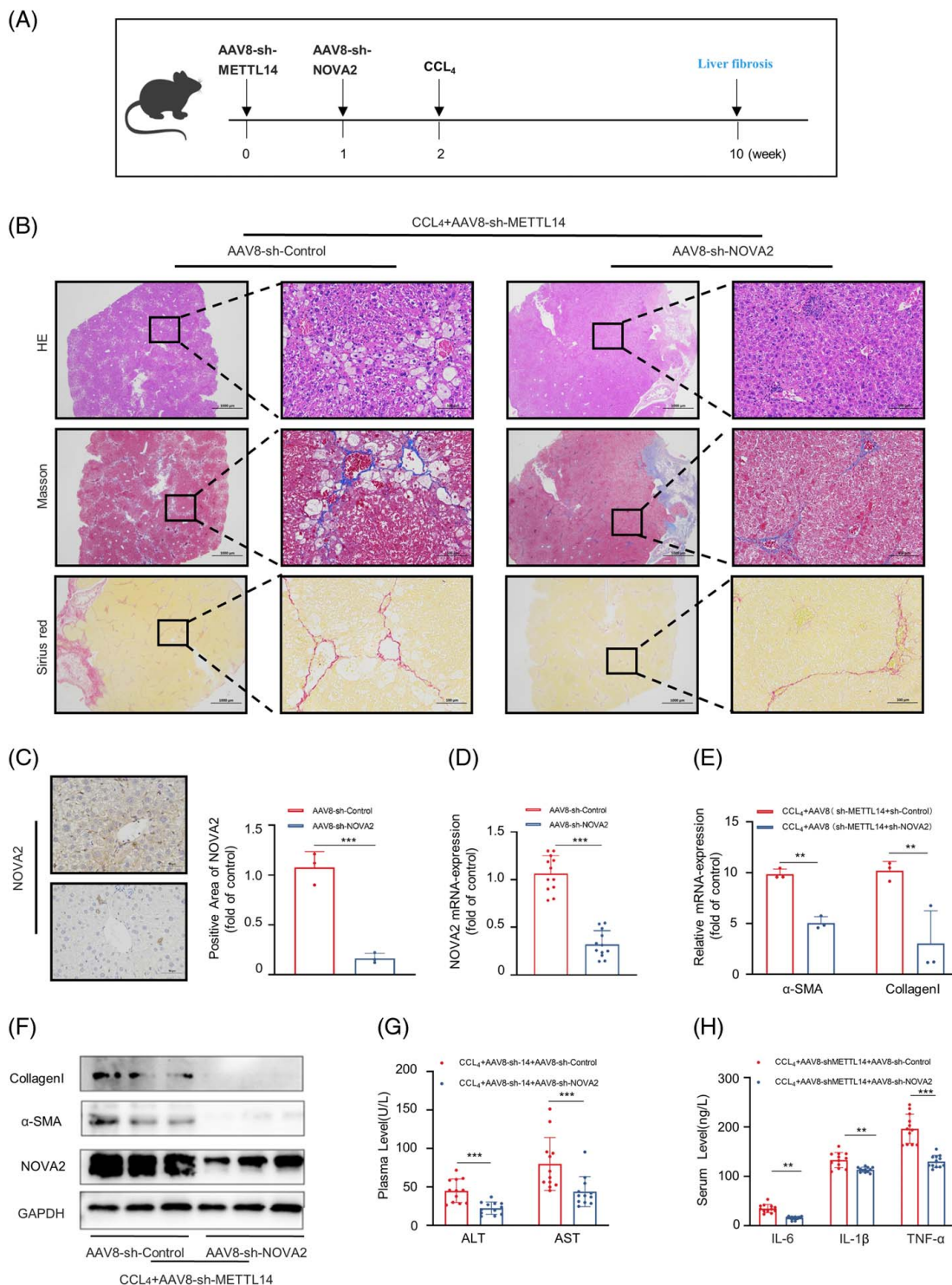


FIGURE 5 METTL14 and NOVA2 regulate the activation of HSCs. (A, B) ECM deposition after transfection with sh-METTL14 or cotransfected sh-METTL14 and si-NOVA2 in LX2 cells and primary HSCs. (C, D) Proliferation ability after transfection with sh-METTL14 or cotransfected sh-METTL14 and si-NOVA2 in LX2 cells and primary HSCs. (E) Apoptosis status after transfection with sh-METTL14 or cotransfected sh-METTL14 and si-NOVA2 in LX2 cells and primary HSCs. (F) METTL14 and NOVA2 regulate LF progression by modulating the Wnt/ β -catenin signaling pathway. Data are presented as the mean \pm SD. * $p < 0.05$; ** $p < 0.01$; and *** $p < 0.001$ (Student t test). Abbreviations: ECM, extracellular matrix; NOVA2, neuro-oncological ventral antigen 2.



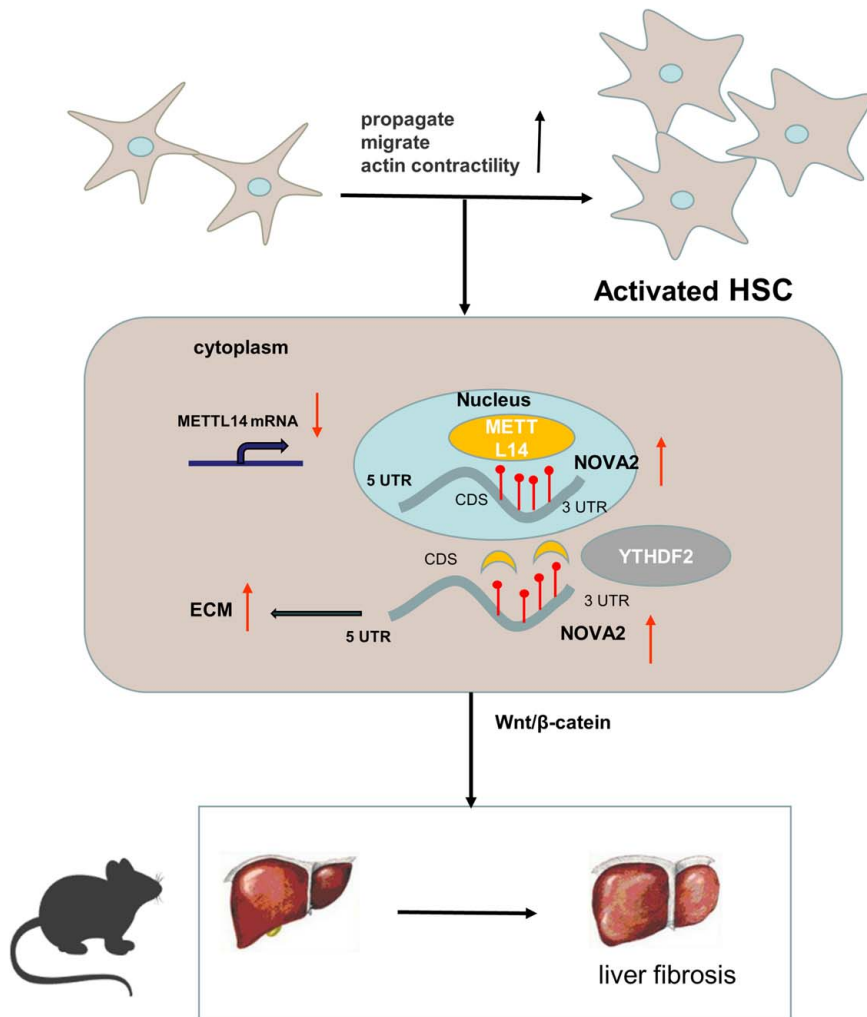


FIGURE 7 The graphic illustration of this study. METTL14 exerts m⁶A modification on NOVA2 mRNA via directly binding to its 3'UTR region in nucleus. Then the m⁶A modified NOVA2 mRNA is recognized by YTHDF2 in cytoplasm and degraded by YTHDF2. Taken together, the METTL14-YTHDF2-NOVA2 axis regulates LF progression. Abbreviation: ECM, extracellular matrix; m⁶A, N⁶-methyladenosine; NOVA2, neuro-oncological ventral antigen 2.

METTL14 regulates NOVA2 mRNA stability through a pathway reliant on an m⁶A-YTHDF2

MeRIP-qPCR was conducted in LX2 cell lines and primary HSCs to confirm whether METTL14-mediated m⁶A modification targeted NOVA2. Knocking down METTL14 remarkably reduced the m⁶A enrichment of NOVA2 (Figure 4A, B). In addition, the mRNA and protein levels of NOVA2 were shown to be higher in METTL14 knockdown cells and lower in METTL14 overexpression cells (Figure 4C, D). In combination with the prediction website SRAMP (<http://www.cuilab.cn/sramp/>), we found that four motif sites existed in this fragment. We employed the site sequence to establish the wild-type and mutant NOVA2 reporter gene (Figure 4E). We discovered that METTL14 affected the expression of NOVA2 through the motif sequence at recognition site 907 (Figure 5F). To either

elevate or lower gene expression, the m⁶A methylation added by m⁶A writers needs to be recognized by m⁶A readers. Of these, YTHDF2 is an mRNA degradation-promoting modulator that may be recruited by METTL14 to facilitate NOVA2 mRNA decay. To test this hypothesis, we first used targeted siRNA to knockdown YTHDF2 (Figure 4G) and discovered that mRNA and protein levels of NOVA2 were increased (Figure 4H). In addition, to establish whether YTHDF2 binds to NOVA2 mRNA in a direct manner, we performed RIP tests. The RIP tests illustrated that the groups with antibodies against YTHDF2 bound significantly more NOVA2 mRNA in LX2 and primary HSCs than those with antibodies against IgG (Figure 4I). Furthermore, the results of the RNA stability experiments showed that the NOVA2 decay rate displayed a considerably slower tendency following treatment with siRNA-targeted YTHDF2 (Figure 4J, K). These results show that YTHDF2 can

identify METTL14-methylated NOVA2 mRNA and speed up its decay.

Progress of regulation of LF by NOVA2 and METTL14

Despite the established significance of METTL14 in LF advancement, it was not known whether or not the impact was specifically due to NOVA2, the target gene for m⁶A modification. Rescue studies were performed to determine whether NOVA2 knockdown might reverse the influence of METTL14 knockdown, providing insight into the potential significance of NOVA2 as the target gene of METTL14 in the advancement of LF. Remarkably, the results demonstrated that, after downregulating NOVA2 (Supplemental Figure S7E, F, <http://links.lww.com/HC9/A450>), the elevated ECM level generated by sh-METTL14 was greatly attenuated (Figure 5A, B). Moreover, knocking down NOVA2 expression considerably lowered the high proliferative (Figure 5C, D) and migratory (Supplemental Figure S5B, <http://links.lww.com/HC9/A448>) rates induced by sh-METTL14. Knocking down NOVA2 significantly reduced F-actin contractility induced by knocking down METTL14 (Supplemental Figure S6B, <http://links.lww.com/HC9/A449>). We also discovered that METTL14 could control the Wnt/ β -catenin pathway by modulating the NOVA2 expression (Figure 5F), which affects the development of LF. To confirm the involvement of NOVA2 in LF progression, we conducted *in vivo* experiments in mice using tail vein injections of AAV8-sh-NOVA2 (Figure 6A). The NOVA2 knockdown mouse model had been successfully established (Figure 6B–D). Data analysis showed that AAV8-sh-NOVA2 significantly reduced ECM deposition (Figure 6E, F), transaminase levels (Figure 6G), and serum inflammatory factor levels (Figure 6H) in the liver of a fibrotic mouse model with low expression of METTL14. These findings further suggest that NOVA2 may alleviate the exacerbation of LF caused by AAV8-sh-METTL14.

DISCUSSION

LF has emerged as a significant global health issue, owing to its rising incidence and the absence of specific and effective therapies, for which there currently exist no viable options. Unless effectively treated, LF causes the formation of fibrous nodules in the liver, disrupts normal liver function and structure, and ultimately leads to liver cirrhosis, which may worsen liver function or possibly cause liver cancer.^[16] Therefore, understanding the pathogenesis of LF and finding ways to treat it are urgent research priorities. The internal modification known as m⁶A is the most prevalent, abundant, and conserved form of internal modification in mammalian mRNA.^[17–20] There

is mounting evidence that m⁶A modification performs a critical role in controlling a wide range of biological processes, such as cell fate determination, differentiation, pluripotency, and metabolism. The function of m⁶A modification in LF, however, is still debatable. Previous studies have proved that, in the process of iron death in HSCs, m⁶A modification increases, and with the increase in METTL3 and METTL14 expressions, the FTO expression level decreases.^[21,22] However, recent studies have proved that the activation of HSCs is accompanied by the increase of m⁶A level, and the attenuation in HSC activation and LF is the outcome of METTL3 deficiency.^[23] Further investigations will be required to better address this controversy.

METTL14 is a crucial m⁶A writer, and we show for the first time that it performs a fundamental function in LF advancement. This study supports these findings in several ways. We began by performing a bioinformatics analysis of previously collected LF data. In multiple data sets of the GEO database, the expression of METTL14 in LF patients was decreased. We collected liver biopsy specimens of LF patients and found that the expression of METTL14 was decreased compared with the control group by immunohistochemistry. In addition, we found that both activated HSCs cells and mouse LF tissues exhibited lower METTL14 expression levels. Furthermore, *in vivo* and *in vitro* analyses revealed that the overexpression of METTL14 suppresses LF advancement, whereas the knockdown of this gene enhances it. This indicates that METTL14 may be an essential factor in the process of LF. To further explore the molecular mechanism of METTL14 in the progress of LF, we conducted a multiomics sequencing, and the results showed that NOVA2 was a downstream target gene of METTL14. When the METTL14 is knocked down, the degradation of NOVA2 by YTHDF2 is reduced, and the mRNA expression of NOVA2 is increased (Figure 7). Previous studies have found that the deletion or gene knockout of NOVA2 can prevent the normal formation of the vascular lumen.^[24–38] The progression of LF is often accompanied by vascular proliferation, which promotes the activation and proliferation of HSC by furthering the transport of oxygen and nutrients, thus promoting the progress of LF.^[29–32] The point is whether NOVA2 plays a key role in LF. We carried out further research, and the results showed that NOVA2 was highly expressed in the progress of LF. After silencing the expression of NOVA2, we could observe a stagnated growth cycle of HSCs, slow proliferation and migration, weakened F-actin contraction, reduced ECM deposition, and reversed fibrosis. The above results suggested that NOVA2 could promote the development of LF.

It has been identified that NOVA2 is a novel β -catenin RNA-binding protein. The NOVA2 heterodimer positively regulates β -catenin expression by enhancing β -catenin mRNA stability.^[33] The Wnt/ β -catenin signaling pathway is closely linked to cell

self-renewal, proliferation, differentiation, and migration. Its activation is linked to fibrosis in many organ systems, including the lungs, kidneys, heart, skin, and liver.^[34–37] Wnt inhibitors with small molecules are effective in mouse LF models.^[38–40] Based on these results, blocking the Wnt/ β -catenin signaling pathway could be an effective treatment strategy for LF. In this study, we discovered that METTL14 knockdown abnormally activated the Wnt/ β -catenin signaling pathway by modulating the expression status of NOVA2, promoting the development of LF, and potentially providing a new pathogenesis of LF. In animal experiments, we knocked down METTL14 by injecting AAV into the tail vein but, because the AAV targeted the whole liver organ, knocked down METTL14 in the whole liver including the hepatocyte. Previous studies have proved that the deletion of METTL14 can cause the growth cycle of hepatocytes to stagnate in the G1 phase and slow down the proliferation rate.^[41] Moreover, METTL14 can weaken the endoplasmic reticulum stress of hepatocytes, thus reducing the apoptosis of hepatocytes, which has a protective effect on liver cells.^[42] In addition, we found that apoptosis of hepatocytes increased after METTL14 knockdown (Supplemental Figure S8A, B, <http://links.lww.com/HCG9/A451>). Apoptosis of hepatocytes can secrete more inflammatory cytokines, which promotes the activation of HSCs, thus promoting the progress of LF. Our findings add a new epigenetic dimension to the understanding of LF pathogenesis. METTL14 has shown promise as a target for the treatment and prognostic prediction among LF individuals.

AUTHOR CONTRIBUTIONS

Chuanlong Zhu and Xiaoxue Hou designed the research; Xiaoxue Hou, Yuwen Li, Jiali Song, and Linya Peng performed the research; Wenting Li and Jiaying Li collected the clinical samples; Xiaoxue Hou and Linya Peng analyzed data and wrote the article; Wen Zhang and Tiantong Feng checked the statistical calculations; Hui Yuan and Rui Liu commented on and revised the paper. All authors have read and approved the final paper.

ACKNOWLEDGMENTS

The authors thank all the patients enrolled in this study.

FUNDING INFORMATION

This work was supported by the Science and Technology Plan of Hainan Province (Clinical Research Center) (LCYX202103, LCYX202204, and LCYX202306), the Hainan Province Science and Technology Special Fund (ZDYF2022SHFZ067), and the grants from Jiangsu Provincial Medical Key Discipline (Laboratory) Cultivation Unit and Hainan Province Clinical Medical Center.

CONFLICTS OF INTEREST

The authors have no conflicts to report.

DATA AVAILABILITY STATEMENT

All data generated or analyzed supporting conclusions are included in the current manuscript.

ORCID

Xiaoxue Hou  <https://orcid.org/0000-0003-0065-4867>

Yuwen Li  <https://orcid.org/0009-0008-7673-3987>

Jiali Song  <https://orcid.org/0009-0009-1286-0108>

Linya Peng  <https://orcid.org/0009-0006-0243-0583>

Wen Zhang  <https://orcid.org/0000-0002-9474-9359>

Rui Liu  <https://orcid.org/0000-0002-9962-6980>

Hui Yuan  <https://orcid.org/0000-0001-8533-260X>

Tiantong Feng  <https://orcid.org/0009-0006-0673-0006>

Jiaying Li  <https://orcid.org/0009-0000-3981-5694>

Wenting Li  <https://orcid.org/0000-0001-7734-4838>

Chuanlong Zhu  <https://orcid.org/0000-0001-6557-1654>

REFERENCES

- Gines P, Krag A, Abraldes JG, Sola E, Fabrellas N, Kamath PS. Liver cirrhosis. *Lancet*. 2021;398:1359–76.
- Long B, Koyfman A. The emergency medicine evaluation and management of the patient with cirrhosis. *Am J Emerg Med*. 2018;36:689–98.
- Kisseleva T, Brenner D. Molecular and cellular mechanisms of liver fibrosis and its regression. *Nat Rev Gastroenterol Hepatol*. 2021;18:151–66.
- Gao J, Wei B, de Assuncao TM, Liu Z, Hu X, Ibrahim S, et al. Hepatic stellate cell autophagy inhibits extracellular vesicle release to attenuate liver fibrosis. *J Hepatol*. 2020;73:1144–54.
- Garbuzenko DV. Pathophysiological mechanisms of hepatic stellate cells activation in liver fibrosis. *World J Clin Cases*. 2022;10:3662–76.
- Kisseleva T, Brenner DA. Hepatic stellate cells and the reversal of fibrosis. *J Gastroenterol Hepatol*. 2006;21(suppl 3):S84–7.
- Lewis CJ, Pan T, Kalsotra ARNA. modifications and structures cooperate to guide RNA-protein interactions. *Nat Rev Mol Cell Biol*. 2017;18:202–10.
- Liu F, Zhang X, Liu Z, Cai W, Song C, Jiang Y, et al. M(6)A modifier-mediated methylation characterized by diverse prognosis, tumor microenvironment, and immunotherapy response in hepatocellular carcinoma. *J Oncol*. 2022;2022:2513813.
- Yang Y, Hsu PJ, Chen YS, Yang YG. Dynamic transcriptomic m(6)A decoration: writers, erasers, readers and functions in RNA metabolism. *Cell Res*. 2018;28:616–24.
- Xue T, Qiu X, Liu H, Gan C, Tan Z, Xie Y, et al. Epigenetic regulation in fibrosis progress. *Pharmacol Res*. 2021;173:105910.
- Patil DP, Pickering BF, Jaffrey SR. Reading m(6)A in the transcriptome: m(6)A-binding proteins. *Trends Cell Biol*. 2018;28:113–27.
- Zhang J, Huang P, Wang D, Yang W, Lu J, Zhu Y, et al. m(6)A modification regulates lung fibroblast-to-myofibroblast transition through modulating KCN H6 mRNA translation. *Mol Ther*. 2021;29:3436–48.
- Pradella D, Deflorian G, Pezzotta A, Di Matteo A, Belloni E, Campolungo D, et al. A ligand-insensitive UNC5B splicing

- isoform regulates angiogenesis by promoting apoptosis. *Nat Commun.* 2021;12:4872.
14. Xiao H. MiR-7-5p suppresses tumor metastasis of non-small cell lung cancer by targeting NOVA2. *Cell Mol Biol Lett.* 2019; 24:60.
 15. Gallo S, Arcidiacono MV, Tisato V, Piva R, Penolazzi L, Bosi C, et al. Upregulation of the alternative splicing factor NOVA2 in colorectal cancer vasculature. *Onco Targets Ther.* 2018;11: 6049–56.
 16. Lua I, Li Y, Zagory JA, Wang KS, French SW, Sévigny J, et al. Characterization of hepatic stellate cells, portal fibroblasts, and mesothelial cells in normal and fibrotic livers. *J Hepatol.* 2016;64: 1137–46.
 17. Zhao BS, Wang X, Beadell AV, Lu Z, Shi H, Kuuspalu A, et al. m(6)A-dependent maternal mRNA clearance facilitates zebrafish maternal-to-zygotic transition. *Nature.* 2017;542:475–8.
 18. O'Reilly S. Epigenetics in fibrosis. *Mol Aspects Med.* 2017;54: 89–102.
 19. Ma W, Wu T. RNA m6A modification in liver biology and its implication in hepatic diseases and carcinogenesis. *Am J Physiol Cell Physiol.* 2022;323:C1190–205.
 20. Yang L, Liu Y, Sun Y, Huang C, Li J, Wang Y. New advances of DNA/RNA methylation modification in liver fibrosis. *Cell Signal.* 2022;92:110224.
 21. Shen M, Li Y, Wang Y, Shao J, Zhang F, Yin G, et al. N(6)-methyladenosine modification regulates ferroptosis through autophagy signaling pathway in hepatic stellate cells. *Redox Biol.* 2021;47:102151.
 22. Shen M, Guo M, Li Y, Wang Y, Qiu Y, Shao J, et al. m(6)A methylation is required for dihydroartemisinin to alleviate liver fibrosis by inducing ferroptosis in hepatic stellate cells. *Free Radic Biol Med.* 2022;182:246–59.
 23. Li Y, Kang X, Zhou Z, Pan L, Chen H, Liang X, et al. The m(6) A methyltransferase Mettl3 deficiency attenuates hepatic stellate cell activation and liver fibrosis. *Mol Ther.* 2022;30: 3714–28.
 24. Li F, Xiong Y, Yang M, Chen P, Zhang J, Wang Q, et al. c-Mpl-del, a c-Mpl alternative splicing isoform, promotes AMKL progression and chemoresistance. *Cell Death Dis.* 2022;13:869.
 25. Liu J, Deng W, Xiao Z, Huang X, Lin M, Long Z. Identification of RNA modification-associated alternative splicing signature as an independent factor in head and neck squamous cell carcinoma. *J Immunol Res.* 2022;2022:8976179.
 26. Zhang QX, Pan YM, Xiao HL, An N, Deng SS, Du X. Alternative splicing analysis showed the splicing factor polypyrimidine tract-binding protein 1 as a potential target in acute myeloid leukemia therapy. *Neoplasma.* 2022;69:1198–208.
 27. Angiolini F, Belloni E, Giordano M, Campioni M, Forneris F, Paronetto MP, et al. A novel L1CAM isoform with angiogenic activity generated by NOVA2-mediated alternative splicing. *Elife.* 2019;8:e44305.
 28. Giampietro C, Deflorian G, Gallo S, Di Matteo A, Pradella D, Bonomi S, et al. The alternative splicing factor Nova2 regulates vascular development and lumen formation. *Nat Commun.* 2015; 6:8479.
 29. Yang L, Yue W, Zhang H, Zhang Z, Xue R, Dong C, et al. Dual targeting of angiotensin-1 and von Willebrand factor by micro-RNA-671-5p attenuates liver angiogenesis and fibrosis. *Hepatol Commun.* 2022;6:1425–42.
 30. Chen SH, Huang CL, Chiang IP, Chang TC, Wang HW Hsu WF, et al. Liver fibrosis regression correlates with downregulation in liver angiogenesis in chronic hepatitis C through viral eradication. *Eur J Gastroenterol Hepatol.* 2021; 33:1209–7.
 31. Thomas H. Liver: Delineating the role of angiogenesis in liver fibrosis. *Nat Rev Gastroenterol Hepatol.* 2018;15:6.
 32. Lee KC, Hsu WF, Hsieh YC, Chan CC, Yang YY, Huang YH, et al. Dabigatran reduces liver fibrosis in thioacetamide-injured rats. *Dig Dis Sci.* 2019;64:102–2.
 33. Tang S, Zhao Y, He X, Zhu J, Chen S, Wen J, et al. Identification of NOVA family proteins as novel beta-catenin RNA-binding proteins that promote epithelial-mesenchymal transition. *RNA Biol.* 2020;17:881–91.
 34. Tewari D, Bawari S, Sharma S, DeLiberto LK, Bishayee A. Targeting the crosstalk between canonical Wnt/beta-catenin and inflammatory signaling cascades: a novel strategy for cancer prevention and therapy. *Pharmacol Ther.* 2021;227: 107876.
 35. Wang J, Li L, Li L, Yan Q, Li J, Xu T. Emerging role and therapeutic implication of Wnt signaling pathways in liver fibrosis. *Gene.* 2018;674:57–69.
 36. Monga SP. beta-catenin signaling and roles in liver homeostasis, injury, and tumorigenesis. *Gastroenterology.* 2015;148:1294–310.
 37. El-Ashmawy NE, Al-Ashmawy GM, Fakhher HE, Khedr NF. The role of WNT/beta-catenin signaling pathway and glutamine metabolism in the pathogenesis of CCl₄-induced liver fibrosis: Repositioning of niclosamide and concerns about lithium. *Cytokine.* 2020;136:155250.
 38. Li W, Zhu C, Li Y, Wu Q, Gao R. Mest attenuates CCl₄-induced liver fibrosis in rats by inhibiting the Wnt/beta-catenin signaling pathway. *Gut Liver.* 2014;8:282–91.
 39. Liu QW, Ying YM, Zhou JX, Zhang WJ, Liu Z, Jia BB, et al. Human amniotic mesenchymal stem cells-derived IGFBP-3, DKK-3, and DKK-1 attenuate liver fibrosis through inhibiting hepatic stellate cell activation by blocking Wnt/beta-catenin signaling pathway in mice. *Stem Cell Res Ther.* 2022;13:224.
 40. Tokunaga Y, Osawa Y, Ohtsuki T, Hayashi Y, Yamaji K, Yamane D, et al. Selective inhibitor of Wnt/beta-catenin/CBP signaling ameliorates hepatitis C virus-induced liver fibrosis in mouse model. *Sci Rep.* 2017;7:325.
 41. Wei J, Harada BT, Lu D, Ma R, Gao B, Xu Y, et al. HRD1-mediated METTL14 degradation regulates m(6)A mRNA modification to suppress ER proteotoxic liver disease. *Mol Cell.* 2021; 81:5052–65. e6.
 42. Cao X, Shu Y, Chen Y, Xu Q, Guo G, Wu Z, et al. Mettl14-mediated m(6)A modification facilitates liver regeneration by maintaining endoplasmic reticulum homeostasis. *Cell Mol Gastroenterol Hepatol.* 2021;12:633–51.

How to cite this article: Hou X, Li Y, Song J, Peng L, Zhang W, Liu R, et al. METTL14 reverses liver fibrosis by inhibiting NOVA2 through an m⁶A-YTHDF2-dependent mechanism. *Hepatol Commun.* 2023;7:e0199. <https://doi.org/10.1097/HC9.000000000000199>